

Analysis of 75 GHz Millimeter Wave Radio over Fiber-Based Fronthaul System for Future Networks

J.D. Gadze¹, R. Akwafo², E.A. Affum³

KNUST, Department of Telecommunication Engineering, College of Engineering, Kumasi, Ghana^{1,2,3}

Abstract: Due to the exponential growth in demand for broadband data, future wireless communication systems will require data rates in the order of 10 Gbits/s and beyond. Currently, as the lower portion of the RF spectrum in the range of 700 MHz to 6 GHz is crowded and limited in bandwidth, it is envisaged that future wireless systems must operate at the higher unlicensed millimeter wave frequencies where vast of unused bandwidth is available. However, due to the short propagation range of mmWaves thus requiring tremendous increase in the number of BS, Radio over Fiber (RoF) technology has been proposed as a major access network solution for future high-bandwidth wireless communication systems. Also, multipath propagation delay spread effects associated with mmWaves have made higher modulation formats such as OFDM etc. stringent requirements for future wireless systems in terms of SNR. Although several works have been done by various researchers at 60, 82 and 110 GHz (characterized with very high attenuation), the purpose of the work done in this paper is to demonstrate the transmission and recovery of a 100 Gbit/s transmission link through OFDM modulation at 75 GHz (characterized by low attenuation) for 5G applications. To the best of our knowledge, this is the first significant work utilizing such mmWave frequency. In this paper, mmWave photonic communication system operating at 75 GHz using LiNb MZM is demonstrated for fiber lengths of up to 35km. The performance of this RoF system has been compared with PSK and QAM encoding formats for both coherent and direct detection systems. However, this work importantly takes into consideration DSP impairment compensation in the receiver system. The performance of the proposed RoF systems is evaluated in terms of QF, BER and the received signal power. The proposed system is modelled and simulated using Optisystem 16.

Keywords: Millimeter wave, Radio over Fiber, Orthogonal Frequency Division Multiplexing, Lithium Niobate MachZender Modulator, Digital Signal Processing.

I. INTRODUCTION

In recent years, the demand for high data rate wireless services by mobile subscribers is ever increasing [1]. To support such an exponential growth in demand, it is envisaged that future wireless communications systems must operate at the higher unlicensed mmWave frequencies [2]. However, as the lower portion of the frequency spectrum is choked by other services, migrating into the mmWave band, where a vast of unused bandwidth is available is an essential solution to solving the spectrum crunch problem. Although mmWaves are capable of providing huge bandwidth, they suffer from short propagation range [3].

This necessitates the need for a large number of BS for an entire coverage area, thereby increasing infrastructural and operational cost. Also, generating mmWave signals at the BS using inexpensive equipment will result in BER degradation [3], [4]. Therefore, the generation and transmission of mmWave signals from a CO to a large number of simplified BS using optical fibers — a technique referred to as Radio over Fiber (RoF) solution (illustrated in Fig.1) — has become a major access network solution proposed for future high bandwidth wireless communication systems [5], [6]-[9].

With this technique, the capacity of wireless communication systems can be increased to overcome the scarcity of bandwidth associated with current wireless systems due to photonic generation of high RF signals and the high bandwidth requirement of optical fibers. Also, higher modulation formats such as OFDM modulation has become a stringent requirement for future wireless broadband systems. This requirement is due to the multi-path spread delay associated with mmWave communication channels.

Therefore, to prepare mm Waves efficiently for transmission to the wireless environment, incorporating OFDM along with RoF has emerged as an efficient way to deal with the issue of multipath delay spread, and to increase robustness against frequency selective fading and narrowband interference. As mentioned, OFDM is a multi-carrier transmission technique [10] that divides the available spectrum into many orthogonal subcarriers, each modulated by a low data rate stream. By doing so, the symbol duration is increased, and the relative amount of dispersion in time caused by multipath delay spread is decreased significantly [11]. Also, the OFDM subcarriers can be modulated by using different M-ary encoding schemes such as Phase Shift Keying (PSK) or Quadrature Amplitude Modulation (QAM) and then carried over a high mmWave carrier. Recently, several research works and papers have been conducted and written by different authors on the integration of RoF with several technologies such as OFDM modulation, WDM etc. in mmWave systems.

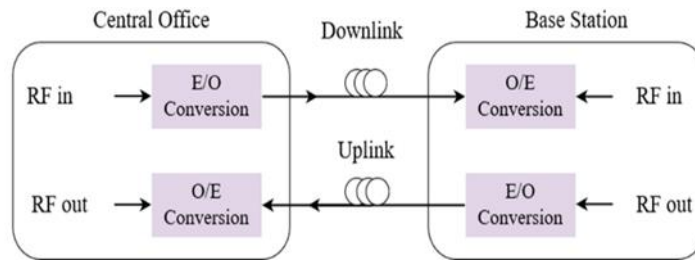


Figure 1. Simple Radio over Fiber system architecture (E/O- Electrical to Optical; O/E-Optical to Electrical)

For instance, the performance of a 40 Gbits/s optical 64-ary QAM-OFDM signal with different number of subcarriers over 100 km SMF has been investigated in [12]. Authors in [13] proposed a 60 GHz RoF link using QAM-OFDM modulation for 40 Gbits/s over a 150 km SMF while using optical CD to configure the base station. Again, in [14], the performance of OFDM modulation in RoF has been investigated and transmitted where 4-ary QAM modulation scheme was used to modulate a bit data rate of 10 Gbits/s over a 100 km fiber transmission link.

Authors in [15] proposed and experimentally demonstrated a hybrid 1.25 Gbits/s QPSK-OFDM RoF transport systems where a 40 GHz mmWave signal was quadrupled from a 10 GHz signal in the optical domain and transported over a 25 km SMF. However, this system showed a BER performance of 5.67×10^{-5} showing low BER performance lower than 10^{-9} . Authors in [16] also have successfully demonstrated a 10 Gbits/s 16-ary QAM OFDM-based RoF system at 7.5 GHz for a SMF length up to 100 km. However, this proposed system showed good QF and BER performance of 32 and 3.07×10^{-63} respectively for the test system bit data rate.

Although the authors of these works have successfully demonstrated multi-Gbits/s RoF links up to 40 Gbits/s, this paper seeks to achieve a 100 Gbits/s RoF link by utilizing 75 GHz mmWave carrier through OFDM modulation and IQ, dispersion and non-linear compensation through digital signal processing. To the best of our knowledge, no significant work has been done utilizing such a mmWave frequency signal.

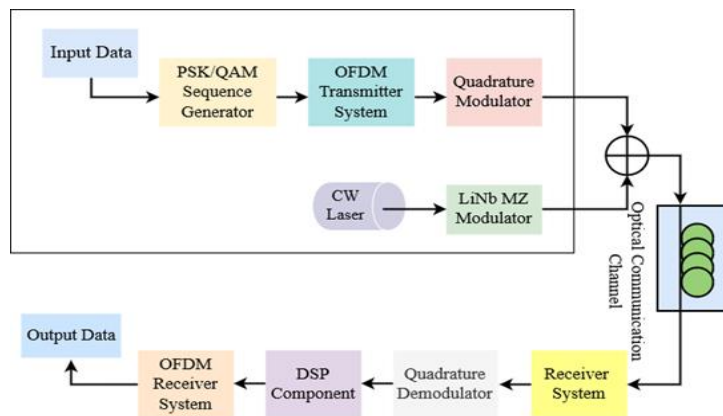


Figure 2. OFDM-based RoF system block diagram

In this paper, we model and simulate a 100 Gbits/s OFDM-based RoF fronthaul system which operates at 75 GHz mmWave frequency with the fiber length varied up to 35 km. In this paper, the proposed OFDM-based RoF systems model uses 16-ary PSK, or 16-ary QAM and or 64-ary QAM with two Low Pass Cosine Roll Off Filters (LP-CROF), a Quadrature Modulator which is used to generate the RF signal and two optical modulators (LiNb MZM) for possible modulation of electrical to optical mode through external intensity modulation at the CO.

Filtering and amplification are used to improve the optically modulated signal. Optical CD or DD technique is used to configure the BS. Also, in this proposed OFDM based system model as shown in figure 2, a DSP component is used to compensate for signal impairment. In this paper, Optisystem 16 is used to model and simulate the proposed OFDM-based RoF system model. A detailed description of the proposed system has been given in section II. The reliability of this proposed system design will be seen from the simulation results in section III.

II. PROPOSED OFDM-BASED ROF SYETEM

The main focus of this paper is to incorporate OFDM modulation technique with different m-ary encoding schemes and DSP into RoF system networks as shown in figure 2. In this OFDM-based RoF system, IQ OFDM signal is generated from an input data in the OFDM transmitter system and up-converted to 75 GHz RF mm-wave frequency using the

quadrature modulator. The input of the OFDM modulator may take any M-ary modulation format such as M-ary PSK or M-ary QAM where M represents the number of symbols. An optical signal from the CW laser source is combined with the electrical IQ OFDM signal and the two waves are modulated by the LiNb MZ modulator. The optical signal formed from combining the waves is launched into the optical fiber channel and converted to an electrical IQ signal by the receiver system. The signal is then down-converted by the quadrature demodulator and the DSP component is used to compensate for signal recovery especially after CD. The resulting electrical IQ signal is received by the OFDM receiver system and the symbols are demodulated. Figure 3 shows the system architecture and components which was used to implement the proposed system model. This proposed OFDM system model consists of five parts which include; OFDM transmitter system, RF to Optical Up-converter, optical link, Optical to RF down-converter and the OFDM receiver system.

A. OFDM Transmitter System

This section consists of PRBS-Generator used to generate the bit sequence, an M-ary QAM or PSK sequence generator used to generate two parallel M-ary symbol sequences and the OFDM modulator is used to split the data rate into many orthogonal subcarriers each modulated by low-rate data streams.

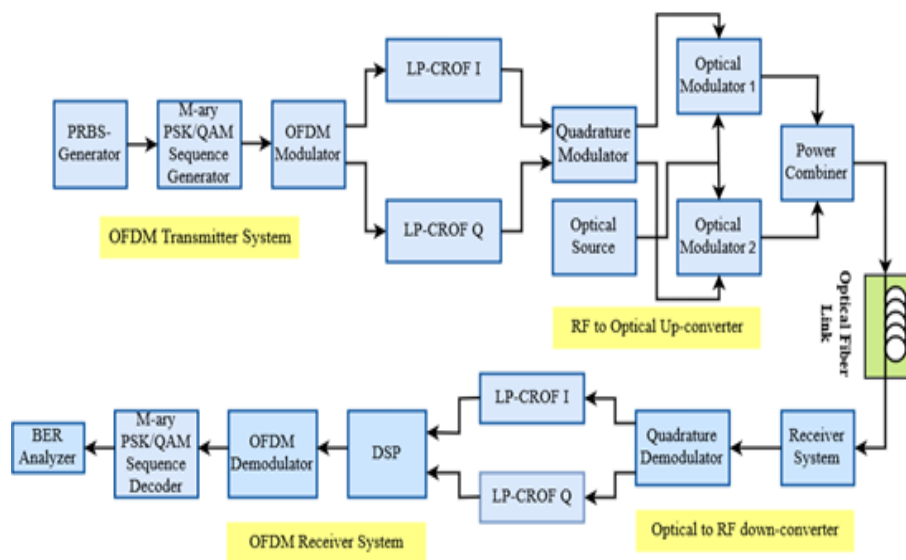


Figure 3. Proposed block diagram of the OFDM based RoF system

In this paper, 512 OFDM subcarriers are used at m-ary QAM positions and the average OFDM power set for the OFDM modulator is 15 dBm with 10 cyclic prefix pints. The output I and Q components of the OFDM modulator are filtered by two LP-CROF with a roll off factor of 0.2 and transfer function given as:

$$\omega = \begin{cases} \gamma \\ \sqrt{0.5 \times a^2} \times \left[1 + \cos \left(\frac{|f| - f_1}{r_p \times \Delta f_{FWHM}} \times \pi \right) \right] \\ 0 \end{cases}, \quad \text{where, } z(f) = \begin{cases} \gamma & (|f| < |f_1|) \\ \omega & (f_1 \leq |f| \leq f_2) \\ 0 & (f_2 \leq |f|) \end{cases} \quad (1)$$

where γ is the parameter insertion loss, f_c is the filter cut-off frequency, and r_p is the parameter roll off factor. The parameters f_1 and f_2 are given as:

$$f_1 = 1 - r_p f_c \quad (0 \leq r_p \leq 1) \quad (2)$$

$$f_2 = 1 + r_p f_c \quad (0 \leq r_p \leq 1) \quad (3)$$

The roll off factor of the LP-CROF has a significance impact on the system performance and determines the complexity of the receiver. Also, an ideal gain element with low electrical gain is used to attenuate the signal power. Figure 4 shows the OFDM transmitter system with LP-CROF in optisystem 16.

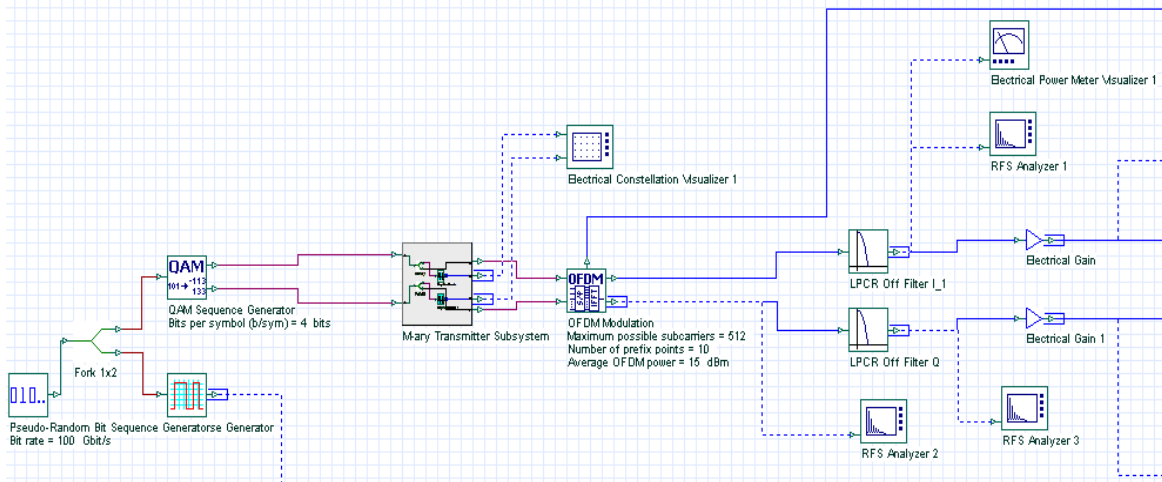


Figure 4. OFDM transmitter system with Low Pass-Cosine Roll Off Filters

B. RF to Optical Up-converter (RTO)

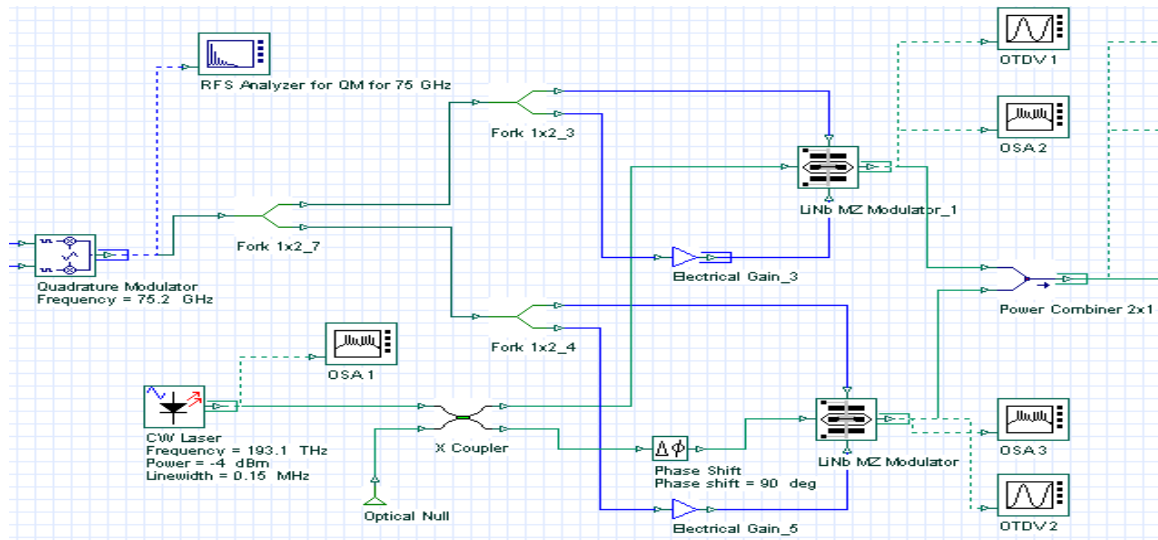


Figure 5. RF to Optical Up-converter system (RTO)

This involves electrical to optical conversion. This section consists of a quadrature modulator which is used to generate any RF signal. In this proposed system, the quadrature modulator was used to generate a 75 GHz RF signal, which is applied to the arms of the two LiNb MZ modulator. For high bit rate light wave systems, the LiNb MZ is an important external modulator used to modulate the RF signal and the optical signal from the continuous wave (CW) laser source with a center frequency of 193.1 THz. This is shown in figure 5.

The average output power of the CW laser is a parameter you specify. In the RTO system, we set a laser launch power of -4dBm. However, the phase noise of the laser is modelled using the Power Density Function, PDF, given in equation 4 as;

$$f(\Delta\phi) = \frac{1}{2\pi\sqrt{\Delta f dt}} \times e^{-\frac{\Delta\phi^2}{4\pi\Delta f dt}} \quad (4)$$

where $\Delta\phi$ is the phase difference between two successive time instants and dt is the time discretization. $2\pi\sqrt{\Delta f}$ has been assumed as a Gaussian random variable with zero mean and variance, with Δf as the laser line-width. The output of the LiNb MZ modulator is given as:

$$E_o(t) = \frac{E_{in}(t)}{10^{(IL/20)}} \times \left[\psi \times e^{(j\pi v_2(t)/V_{\pi RF} + j\pi V_{bias2}/V_{\pi DC})} \right] + \left[(1-\psi) \times e^{(j\pi v_1(t)/V_{\pi RF} + j\pi V_{bias1}/V_{\pi DC})} \right] \quad (5)$$

where $E_{in}(t)$ is the input optical signal, IL is the parameter called Insertion Loss, $v_1(t)$ and $v_2(t)$ are the input electrical voltages for the upper and lower modulator arms, V_{bias1} and V_{bias2} are the setting of the bias voltage 1 and bias voltage 2 of the LiNb MZM, $V_{\pi RF}$ and $V_{\pi DC}$ are the switching modulation voltage and switching bias voltage respectively. ϕ denotes the power splitting ratio of both Y-branch waveguides given by:

$$\phi = \left(1 - \frac{1}{\sqrt{\epsilon_r}}\right) / 2, \text{ where } \epsilon_r = 10^{\text{ExtRatio}/10} \tag{6}$$

ExtRatio is linked to the parameter extinction ratio. The output of the two LiNb MZM is combined using a power combiner.

C. Optical Fiber Communication Link

The system uses a loop control network of SMF, an optical amplifier and a gaussian optical filter to enhance the signal quality. In this paper, the simulation performance of the systems is varied for fiber length up to 35 km. The attenuation coefficient, α is 0.2 dB/km and dispersion of 16.75 ps/nm/km. The scheme for the optical link is shown in figure 6.

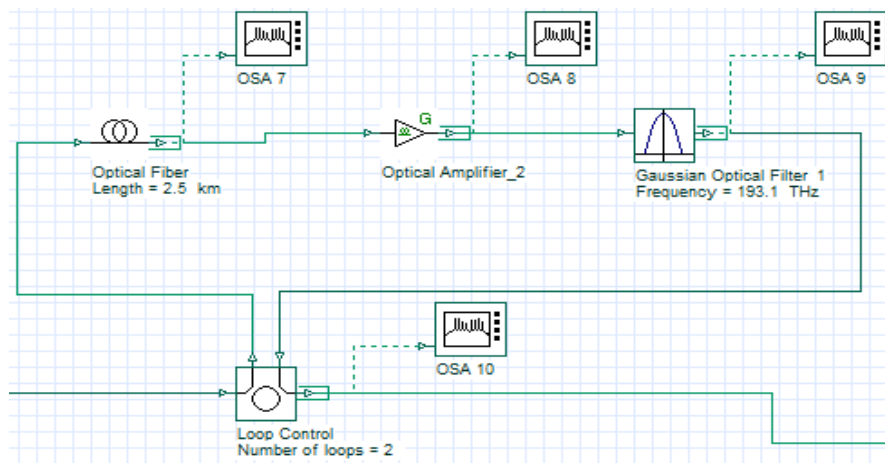


Figure 6. Optical communication link (Optical Fiber Link)

D. Optical to RF Down-converter (OTR)

This section of the system is an optical detector. This paper compares the performance of the system when optical coherent or direct detection is used to implement the OTR. The coherent and direct detector system is shown in figure 7a. and b respectively.

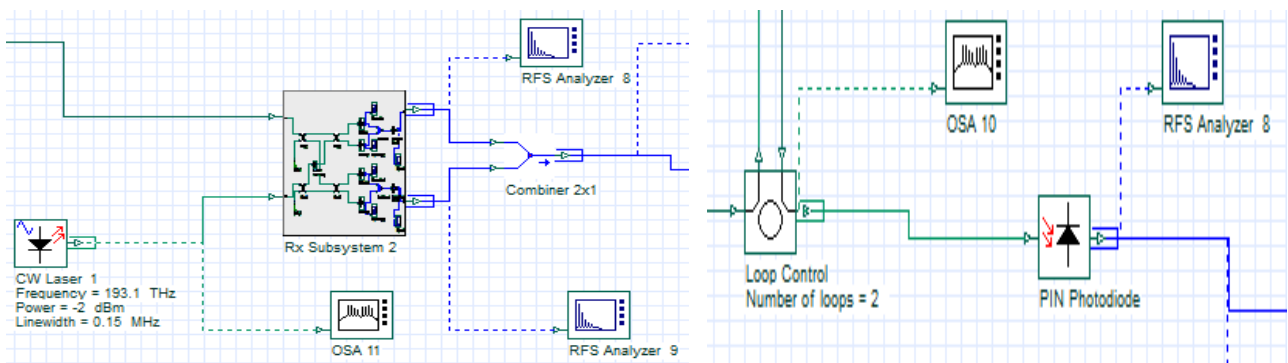


Figure 7. (a) Receiver system with optical coherent detection (b) Receiver system with direct detection

The coherent detector system as shown in figure 7(a), the receiver subsystem (Rx subsystem) consists of two pairs of PIN photo detectors with an external light source produced by a LO with an average power of -2 dBm, while the direct detector system as shown in figure 7(b), uses a single PIN photo detector to convert the optical signal to electrical current. The responsivity of the PIN photo detector is 1 A/W and dark current of 10 nA.

E. OFDM Receiver system

This section of the receiver system consists of a quadrature demodulator which is used to down convert the electrical IQ signal, and is followed by two LP-CROF to filter the I and Q signal components. The DSP component in the receiver system is used to remove the need for dynamic polarization control and to compensate for linear (and some extent of non-linearity) transmission impairments [17], and also to mitigate amplitude and phase imbalances within the IQ signals and fiber dispersion which aids the recovery of the signal especially in coherent detection systems. These imbalances may occur from inappropriate bias voltage settings for the modulators, photodetector responsivity mismatches, and misalignment of the polarization controller. Figure 8. shows the OFDM receiver system with DSP compensation.

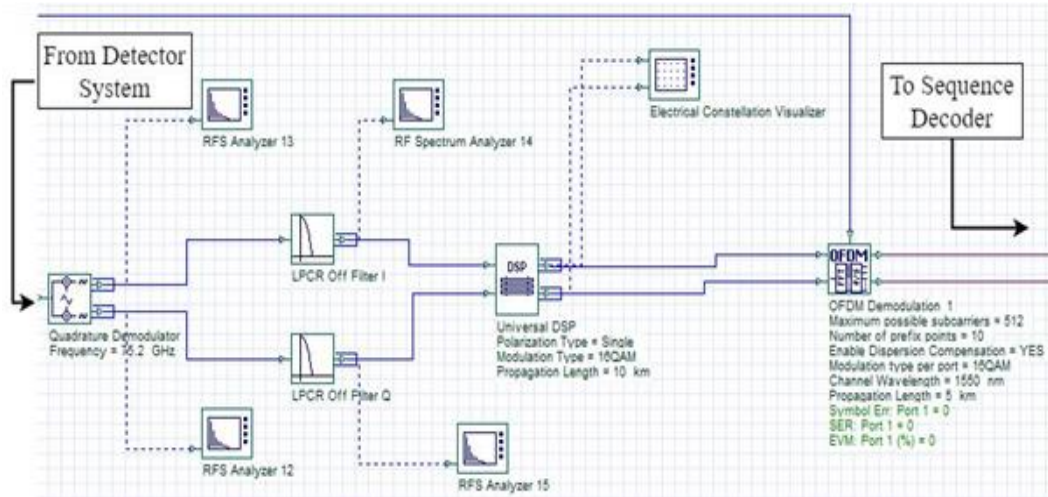


Figure 8. OFDM receiver system with DSP compensation

In this paper, Digital Signal Processing is an important goal to transmit an intended data rate of 100 Gbits/s with high throughput over a varying fiber length from 5 to 35 km. The Gram-Schmidt orthogonalization is used to correct the IQ received signal denoted by $r_1(t)$ and $r_0(t)$, and the GSO results in a new pair of IQ signals denoted by $I^0(t)$ and $Q^0(t)$ given as;

$$I^0(t) = \frac{r_1(t)}{\sqrt{P_1}}, \quad Q(t) = r_0(t) - \frac{\rho \cdot r_1(t)}{\sqrt{P_1}}, \quad Q^0(t) = \frac{Q(t)}{\sqrt{P_0}} \quad (7)$$

where $\rho = E\{r_1(t)r_0(t)\}$ is the correlation coefficient; $P_1 = E\{r_1^2(t)\}$; $P_0 = E\{Q^2(t)\}$ and $E\{\cdot\}$ is the ensemble average operator. Also, the transfer function for the dispersion in frequency domain using a dispersion compensation filter is given as;

$$G(z, \omega) = \exp(-j \cdot \frac{D \cdot \lambda^2 \cdot z}{4 \cdot \pi \cdot c} \cdot \omega^2), \quad (8)$$

where z is the transmission distance, ω is the angular frequency, j is the imaginary unit, λ is the channel wavelength, c is the speed of light, and $D = D_0 + S \times (\lambda - \lambda_0)$ is the dispersion coefficient of the fiber for wavelength λ , S is the dispersion slope, and λ_0 is the reference wavelength. The OFDM demodulator finally is used to demodulate the OFDM symbol.

Figure 9. illustrates the receiver subsystem.

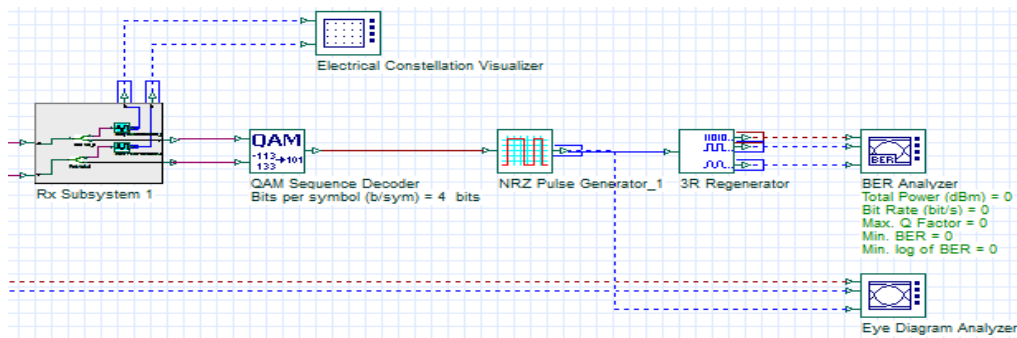


Figure 9. Receiver Subsystem

III. SIMULATION RESULTS AND ANALYSIS

In this section, the simulation results for the proposed OFDM-based RoF system are shown. QAM and PSK modulation formats are used and their performances are compared. The QAM baseband signal uses (4 and 6) bits/symbol and PSK baseband signal uses 4 bits/symbol.

Table 1: Global simulation parameter settings

Parameter	Value
Bit rate	100 Gbits/s
Sequence Length	32768 bits
Number of Sample	131072
Sample per bit	4
Modulation Bandwidth	2 GHz
Number of Subcarriers	512
Fiber Length	5km to 35km
SMF attenuation coefficient	0.2 dB/km

Also, it is important to state that, the same simulation parameters are assumed when the modulation scheme is changed for the two detection systems. The global simulation parameter for the proposed system is shown in table 1.

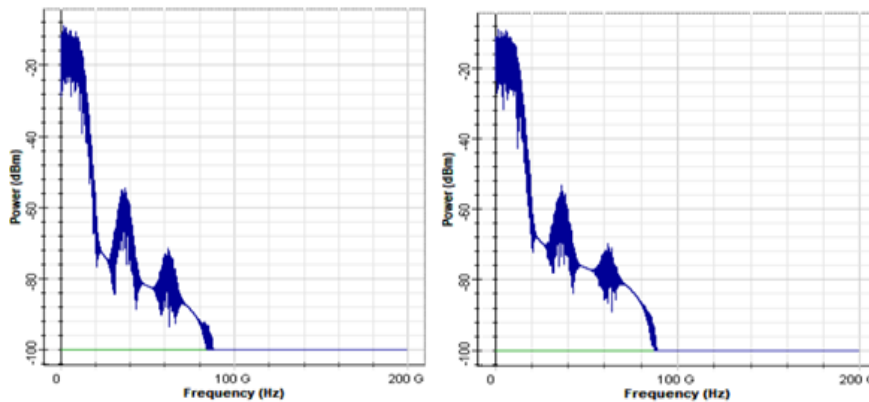


Figure 10. I and Q signal spectrum of the OFDM modulated signal with bit data rate of 100 Gbits/s when 16-ary PSK modulation scheme is used

Figure 10. shows the output spectrum of the I and Q components of the OFDM modulator when 16-ary PSK is used to modulate 100 Gbits/s bit data rate. The RF spectrum analyzer shows a peak OFDM signal power of approximately -5 dBm for the in-phase (I) and quadrature (Q) signal components. However, we observe that a change in the modulation scheme changes the spectrum bandwidth of the OFDM modulated signal. Figure 11 and 12 respectively, illustrate the OFDM-modulated I and Q signal components for 16 and 64-QAM with OFDM signal power of approximately 40 dBm.

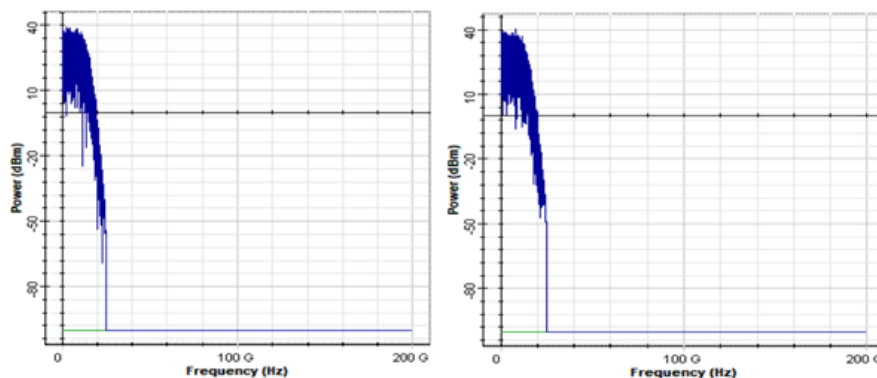


Figure 11. I and Q signal spectrum of the OFDM modulated signal with bit data rate of 100 Gbits/s when 16-ary QAM modulation scheme is used

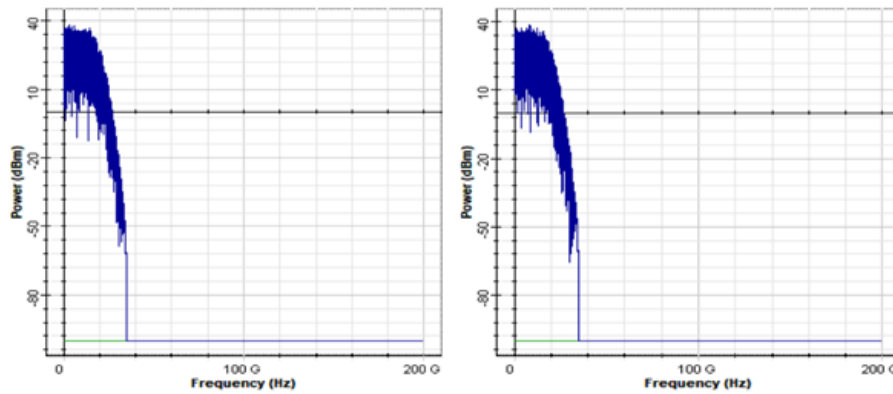


Figure 12. I and Q signal spectrum of the OFDM modulated signal with bit data rate of 100 Gbits/s when 16-ary QAM modulation scheme is used

The up-converted IQ OFDM and time domain signal at 75 GHz is shown in figure 13. for 16-PSK with signal power of -44 dBm. Figure 14 and 15 also show the up-converted signal for 16 and 64-QAM with average signal power of approximately -5 dBm and -3 dBm respectively with varying signal bandwidths. The total output signal of the up-converted RF signal is modulated by the quadrature modulator according to:

$$V_{out} = G [I(t)\cos(2\pi f_c t + \phi_c) - Q(t)\sin(2\pi f_c t + \phi_c)] + b \quad (9)$$

where I and Q are the electrical signals, G is the gain, b is the bias, f_c is the carrier frequency, ϕ_c and is the carrier phase.

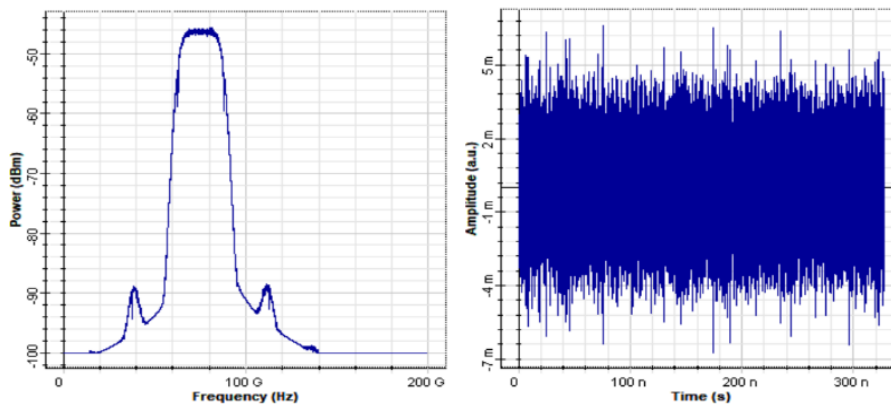


Figure 13. (a) shows the up-converted OFDM signal in frequency domain and (b) shows the up-converted signal in time domain at 75 GHz for 16-PSK

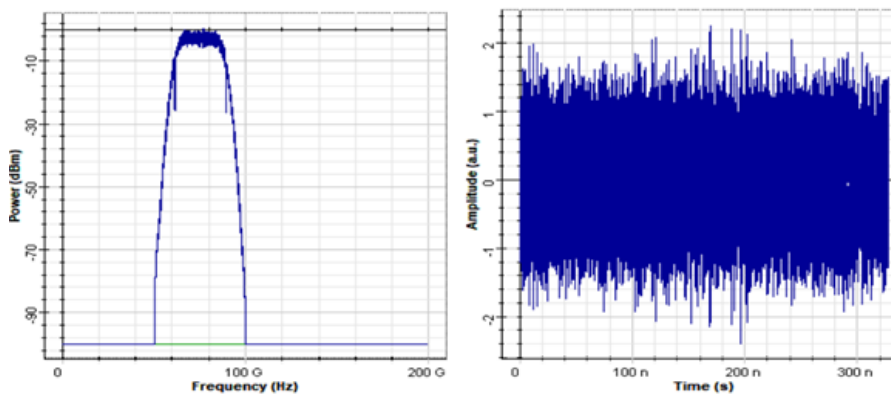


Figure 14. (a) shows the up-converted OFDM signal in frequency domain and (b) shows the up-converted signal in time domain at 75 GHz for 16-QAM

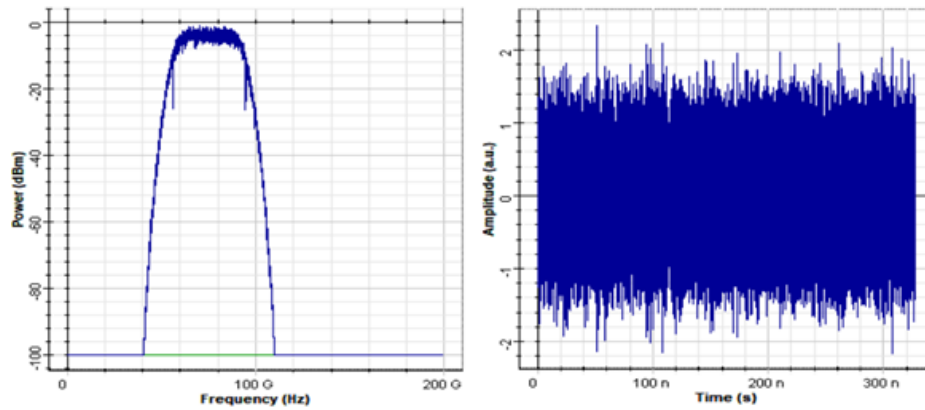


Figure 15. (a) shows the up-converted OFDM signal in frequency domain and (b) shows the up-converted signal in time domain at 75 GHz for 64-QAM

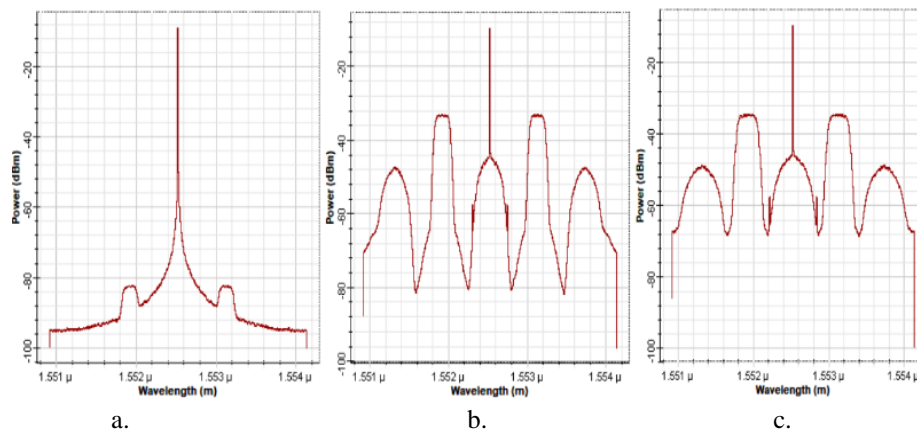


Figure 16. Optical modulated signal for (a) 16-PSK, (b) 16-QAM and (c) 64-QAM

Figure 16, however, illustrates the optical modulated spectrum respectively for 16-PSK, 16-QAM and 64-QAM. The spectrums show poor quality with high harmonics especially for 16 and 64-QAM when the RF-OFDM signal is modulated by the two LiNb MZ modulators. The spectrum shows signal harmonics with high harmonic power levels at the sidebands of the signal. The output spectral quality of the LiNb MZ modulator was enhanced through filtering and amplification of the signal. Figure 17. illustrates the improved, filtered and amplified spectrums for the various modulation schemes from the optical transmission loop network of a 5 km fiber length. The spectrums however show noise power of approximately -37 dBm with variations in peak power.

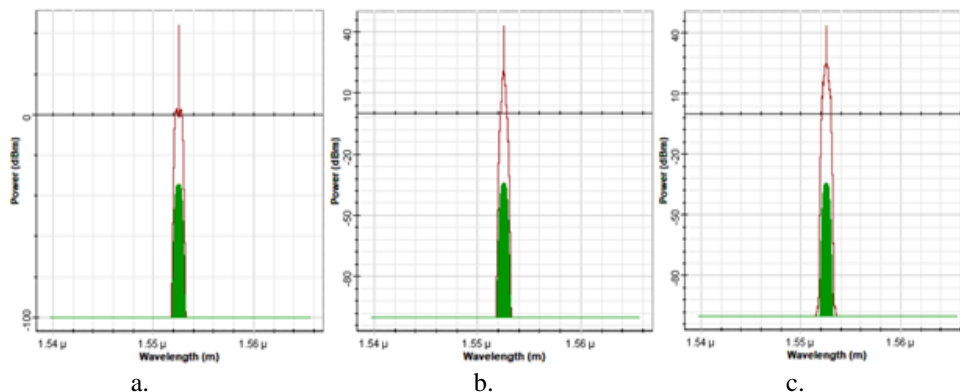


Figure 17. Output signal spectrums for (a) 16-PSK, (b) 16-QAM and (c) 64-QAM

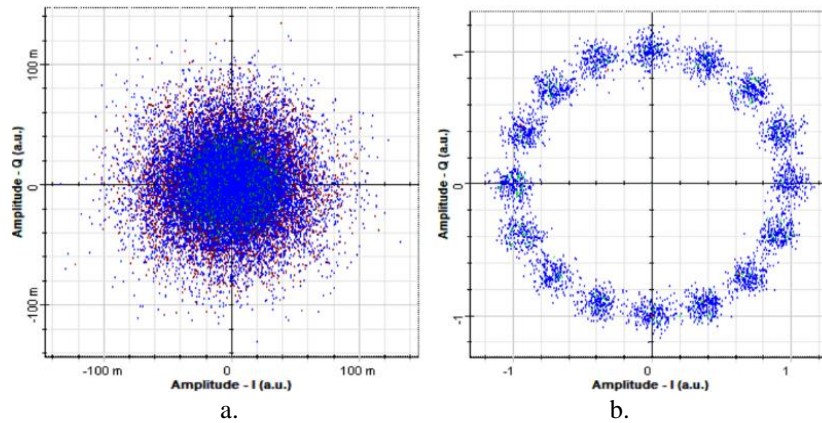


Figure 18. (a) RF-OFDM signal after dispersion compensation using 16-PSK scheme with coherent detection at the receiver and (b) Carrier Phase Estimation for 16-PSK with coherent detection using DSP compensation for a 5 km fiber length

The demodulated OFDM symbols at the receiver system are shown on the electrical constellation diagrams for 16-PSK, 16-QAM and 64-QAM modulation formats when either coherent or direct detection systems are used to configure the receiver system. The performance of these modulation formats is summarized in tables in terms of BER and quality factor. The results shown are reported for 100 Gbits/s bit data rate while using a modulation bandwidth of 2 GHz and 512 subcarriers.

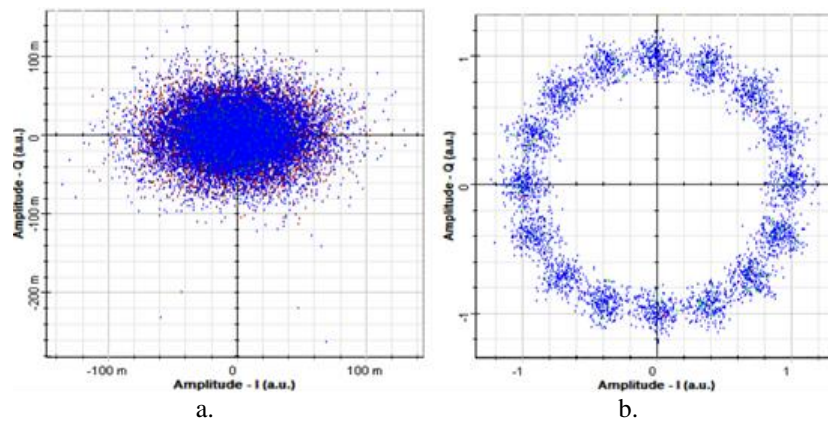


Figure 19. (a) RF-OFDM signal after dispersion compensation using 16-PSK scheme with direct detection at the receiver and (b) Carrier Phase Estimation for 16-PSK direct detection using DSP compensation for a 5 km fiber length

However, in this paper the results are reported for a case without DSP compensation, and a case when DSP is used in the receiver system to compensate for bit errors. In figure 19, we show the demodulated OFDM signal after dispersion compensation and baseband modulation for 16-PSK scheme with optical coherent detection for a 5 km fiber length using DSP compensation. The signal is useful and can be decoded by a user. Table 2 shows a summary of the QF and BER values of the system. Figure 19, however illustrates the constellation diagram for the demodulated OFDM signal when direct detection is implemented using DSP compensation for 16-PSK. The constellation shows that the demodulated OFDM signal is useful and can be decoded by a user as this system meets the minimum BER requirement of 10^{-9} .

Table 2: Summary of QF and BER for 16-PSK with coherent detection using DSP compensation

Distance (km)	Quality Factor	Min BER	Log (Min BER)
5	7.46	41.73×10^{-15}	-13.38
10	6.82	2.05×10^{-12}	-11.69
20	5.59	6.73×10^{-9}	-8.17
35	4.43	1.54×10^{-6}	-5.81

Table 3: Summary of QF and BER for 16-PSK with direct detection using DSP compensation

Distance (km)	Quality Factor	Min BER	Log (Min BER)
5	5.51	18.19×10^{-09}	-7.74
10	4.77	1.22×10^{-06}	-5.91
20	3.52	5.79×10^{-05}	-4.24
35	2.68	64.53×10^{-05}	-3.19

In table 2, we observe that the system shows acceptable QF and BER values for fiber length up to 20 km. The system however shows a received signal power of 27.01 dBm when the length of the fiber is 5 km. In table 3, we observe that, the system only shows an acceptable QF and BER value when the length of the fiber is 5 km when direct detection and using DSP compensation is implemented.

Table 4: Summary of QF and BER for 16-PSK with coherent detection without using DSP compensation

Distance (km)	Quality Factor	Min BER	Log (Min BER)
5	5.57	12.90×10^{-09}	-7.89
10	4.94	1.79×10^{-06}	-5.75
20	3.76	7.67×10^{-05}	-4.12
35	3.76	30.86×10^{-05}	-3.51

The system shows unacceptable QF and BER values when the length of the fiber is increased beyond 10 km. The system shows a received signal power of 26.78 dBm. In the case where coherent detection is implemented without using DSP compensation in the receiver system for 16-PSK, the system shows an acceptable QF and BER value for 5 km as illustrated in table 4. Unacceptable QF and BER values are observed for fiber length beyond 5 km. Table 5 shows a summary of the QF and BER values when direct detection is implemented at the receiver without using DSP compensation for 16-PSK. This system however shows unacceptable QF and BER values for all the fiber lengths.

Table 5: Summary of QF and BER for 16-PSK with direct detection without using DSP compensation

Distance (km)	Quality Factor	Min BER	Log (Min BER)
5	3.83	5.21×10^{-05}	-4.28
10	3.17	18.16×10^{-05}	-3.74
20	2.39	0.002310169	-2.64
35	1.15	0.031977416	-1.50

Figure 20. Shows the constellation diagram for 5 km fiber for 16-QAM scheme with coherent detection using DSP compensation at the BS.

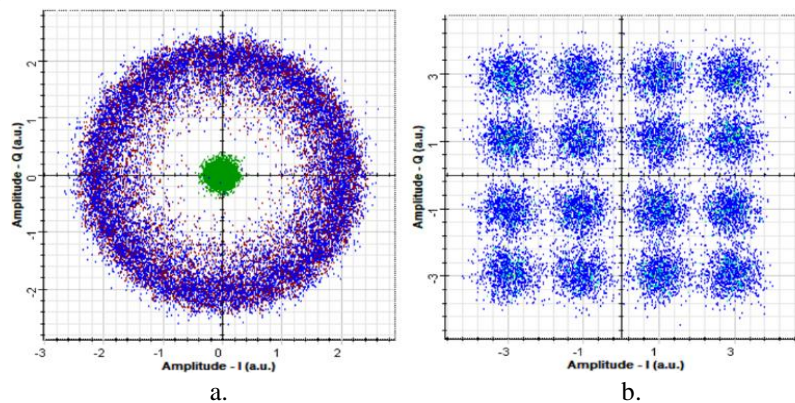


Figure 20. (a) RF-OFDM signal after dispersion compensation using 16-QAM scheme with coherent detection and (b) Carrier Phase Estimation for 16-QAM coherent detection using DSP compensation for 5 km fiber length

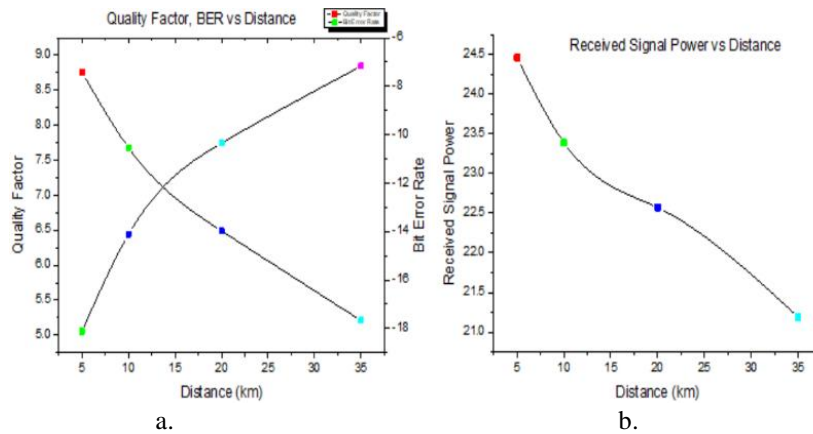


Figure 21. (a) Quality Factor decreases while BER increases when fiber length is increased (b) received signal power decreases when the length of the fiber is increased

The demodulated OFDM signal on the constellation diagram for this system is useful and can be decoded by a user. Table 6 shows a summary of the QF and BER values of the system. This system however shows acceptable QF and BER values for fiber length up to 35 km when DSP compensation is employed in the receiver system as shown in figure 21(a). The system shows a received signal power of 24.46 dBm when the length of the fiber is 5 km. Figure 21(b). shows the relationship between RSP and distance of the system.

Table 6: Summary of QF and BER for 16-QAM with coherent detection using DSP compensation

Distance (km)	Quality Factor	Min BER	Log (Min BER)
5	8.76	0.77×10^{-18}	-18.12
10	7.68	7.81×10^{-15}	-14.11
20	6.49	44.16×10^{-12}	-10.35
35	5.21	67.55×10^{-9}	-7.17

In table 7, the system shows acceptable QF and BER values when direct detection using DSP compensation is implemented for 16-QAM scheme. The system shows acceptable QF and BER values for fiber lengths up to 10 km. The system shows a minimum BER of 10^{-9} when the length of the fiber is 10 km. However, the RSP is 26.8 dBm when the length of the fiber is 5 km. Figure 22. illustrates the constellation diagram for the system at 5 km.

Table 7: Summary of QF and BER for 16-QAM with direct detection using DSP compensation

Distance (km)	Quality Factor	Min BER	Log (Min BER)
5	6.68	11.90×10^{-12}	-10.92
10	5.76	4.08×10^{-9}	-8.39
20	4.89	0.49×10^{-6}	-6.31
35	3.94	67.10×10^{-6}	-4.17

In the case when 16-QAM scheme without using DSP compensation is implemented for coherent detection, the system shows unacceptable QF and BER Values as shown in table 8. As shown in the figure 23, the demodulated signal cannot be used or decoded by a user.

Table 8: Summary of QF and BER for 16-QAM with coherent detection without using DSP compensation

Distance (km)	Quality Factor	Min BER	Log (Min BER)
5	4.79	0.11×10^{-06}	-6.96
10	3.90	2.10×10^{-06}	-5.68
20	2.82	0.0001357709	-3.87
35	1.77	0.0052693257	-2.28

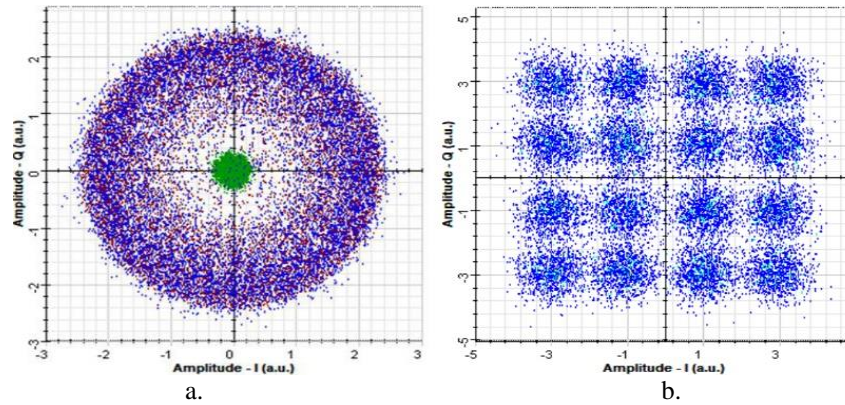


Figure 22. (a) RF-OFDM signal after dispersion compensation using 16-QAM scheme with direct detection and (b) Carrier Phase Estimation for 16-QAM direct detection using DSP compensation for 5 km fiber length

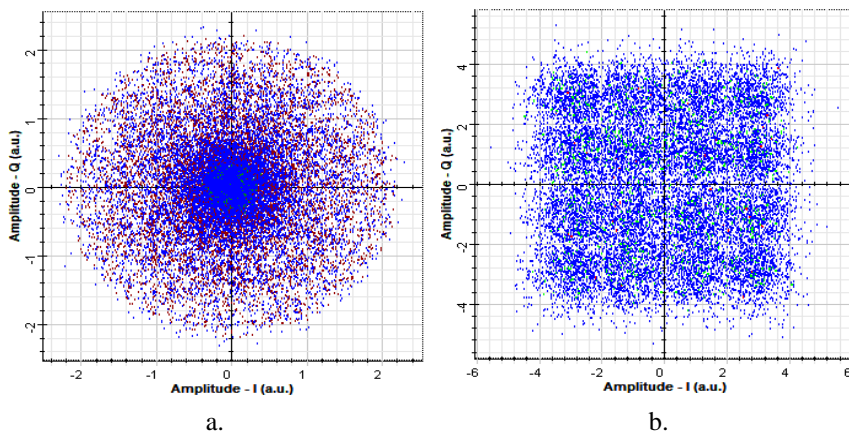


Figure 23. (a) RF-OFDM signal after dispersion compensation using 16-QAM scheme with coherent detection and (b) Carrier Phase Estimation for 16-QAM coherent detection without using DSP compensation for 5 km fiber length

The system again shows degradable QF and BER in table 9 when direct detection is used without DSP compensation in the receiver system for 16-QAM modulation. The demodulated OFDM signal as shown on the constellation diagram in figure 24, however cannot be decoded by a user hence cannot be used.

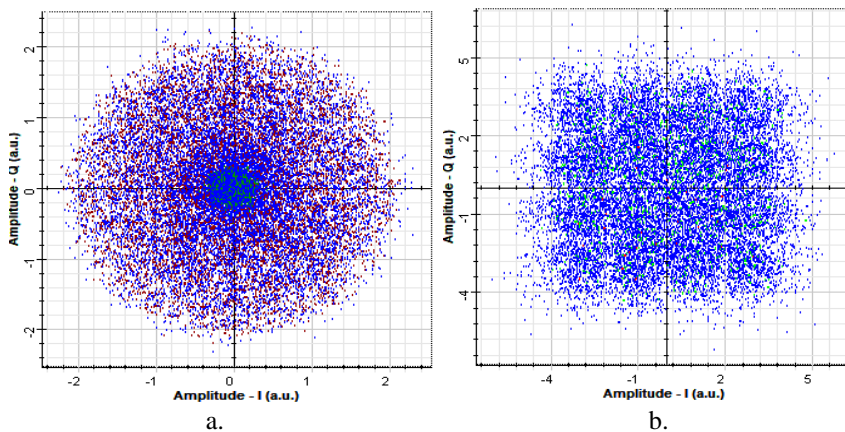


Figure 24. (a) RF-OFDM signal after dispersion compensation using 16-QAM scheme with direct detection and (b) Carrier Phase Estimation for 16-QAM direct detection without using DSP compensation for 5 km fiber length

Table 9: Summary of QF and BER for 16-QAM with direct detection without using DSP compensation

Distance (km)	Quality Factor	Min BER	Log (Min BER)
5	3.53	5.09×10^{-06}	-5.29
10	2.88	0.0002197161	-3.66
20	2.12	0.0026117344	-2.58
35	1.13	0.0237102719	-1.63

However, another case where the number of bits/symbols is 6 (64-QAM) was also investigated for both coherent and direct detection. Implementing DSP compensation in the receiver system for 64-QAM with coherent detection resulted in achieving a very good QF and BER values as shown in the table 10. The systems show highest QF of 13.02 with very good BER value of 2.45×10^{-39} at fiber length of 5 km when DSP compensation is employed in the receiver system.

Table 10: Summary of QF and BER for 64-QAM with coherent detection using DSP compensation

Distance (km)	Quality Factor	Min BER	Log (Min BER)
5	13.02	2.45×10^{-39}	-38.61
10	12.63	12.50×10^{-36}	-34.90
20	11.80	10.37×10^{-33}	-31.98
35	9.60	1.70×10^{-30}	-29.77

A received signal power of 22.96 dBm was observed for this system. The received signal power decreases as the length of the fiber is increased as shown in figure 25(b). Figure 25(a). shows the relationship between the QF, BER and the distance of the fiber. Figure 26. illustrates the constellation diagram for the systems at 5 km.

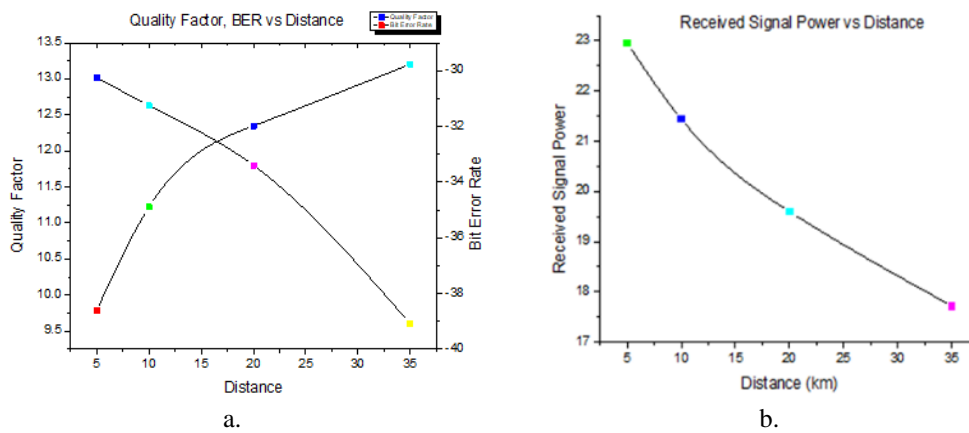


Figure 25. (a) Quality Factor decreases while BER increases when fiber length is increased for 64-QAM with coherent detection (b) received signal power decreases when the length of the fiber is increased

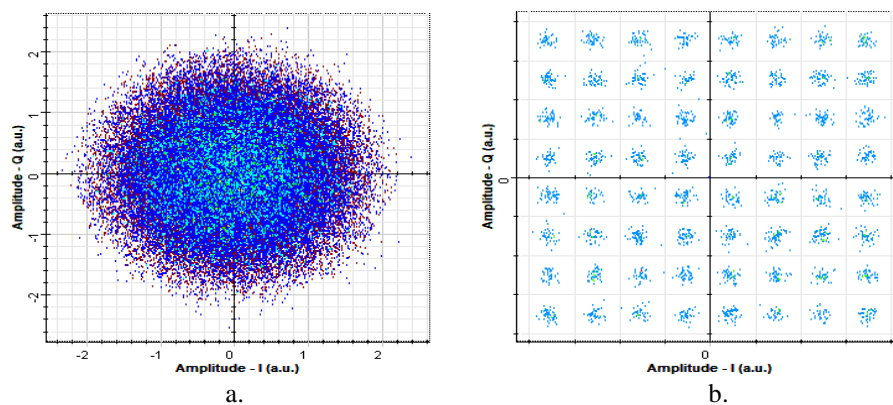


Figure 26. (a) RF-OFDM signal after dispersion compensation using 64-QAM scheme with coherent detection and (b) Carrier Phase Estimation for 64-QAM coherent detection using DSP compensation for 5 km fiber length

In table 11, the QF and BER values decrease when direct detection is used and DSP is implemented to compensate for modulation errors. This system shows acceptable QF and BER values for 5 km to 20 km. An unacceptable QF and BER value is observed for distances beyond 20 km.

Table 11: Summary of QF and BER for 64-QAM with direct detection using DSP compensation

Distance (km)	Quality Factor	Min BER	Log (Min BER)
5	7.40	68.81×10^{-15}	-13.16
10	6.72	0.17×10^{-12}	-12.77
20	5.44	0.41×10^{-9}	-9.39
35	4.26	17.82×10^{-6}	-4.75

The received signal power of this system is 24.88 dBm. Figure 27. illustrates the constellation diagram for the system when direct detection is implemented in the receiver and the length of the fiber is 5 km. The demodulated OFDM signal is useful and can be decoded by a user. Figure 28(b). shows the relationship between the received signal power and the distance of the fiber. In the case where coherent detection is implemented without using DSP compensation, the QF and BER further decrease with QF and BER of 6.48 and 1.50×10^{-12} respectively for a 5 km fiber length.

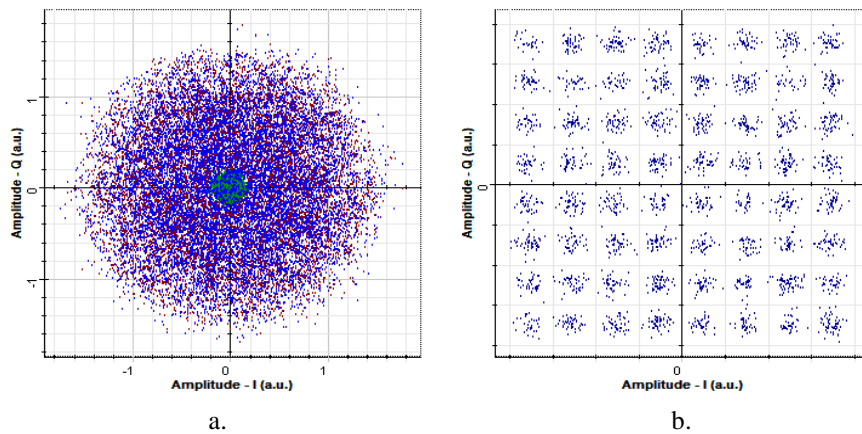


Figure 27. (a) RF-OFDM signal after dispersion compensation using 64-QAM scheme with direct detection and (b) Carrier Phase Estimation for 64-QAM direct detection using DSP compensation for 5 km fiber length

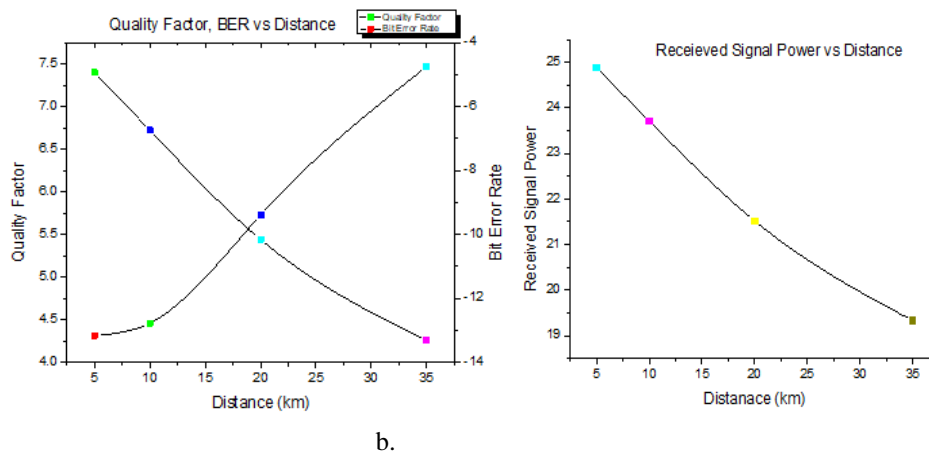
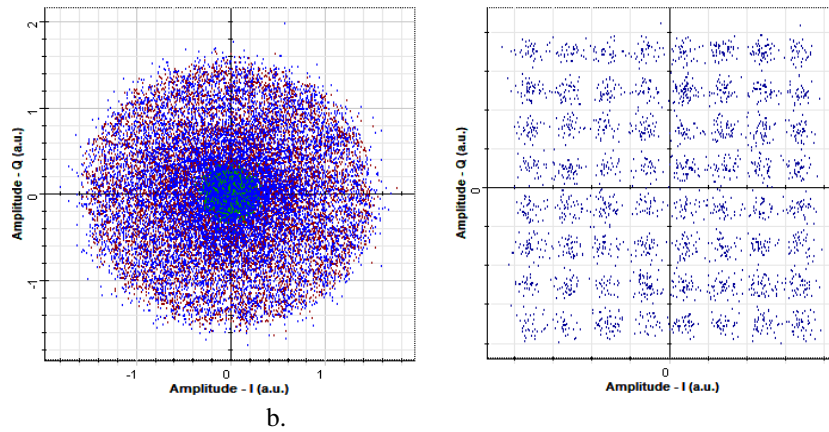


Figure 28. (a) Quality Factor decreases while BER increases when fiber length is increased for 64-QAM with direct detection (b) received signal power decreases when the length of the fiber is increased

The system however shows unacceptable values when the length of the fiber is increased beyond 10 km as shown in table 12. The systems show a received signal power of 22.19 dBm at 5 km. Figure 29. illustrates the constellation diagram of the demodulated OFDM signal of the system. As shown from the constellation, the signal is useful and the signal can be decoded by a user. However, using 64-QAM modulation scheme and implementing direct detection without DSP resulted



a. b.
Figure 29. (a) RF-OFDM signal after dispersion compensation using 64-QAM scheme with coherent detection and (b) Carrier Phase Estimation for 64-QAM coherent detection without using DSP compensation for 5km fiber length

in achieving an acceptable QF and BER value for only 5 km fiber length. This system shows unacceptable performance values for the fiber lengths beyond 5 km as shown in table 13. The received signal power for this system at 5 km is 24.28 dBm.

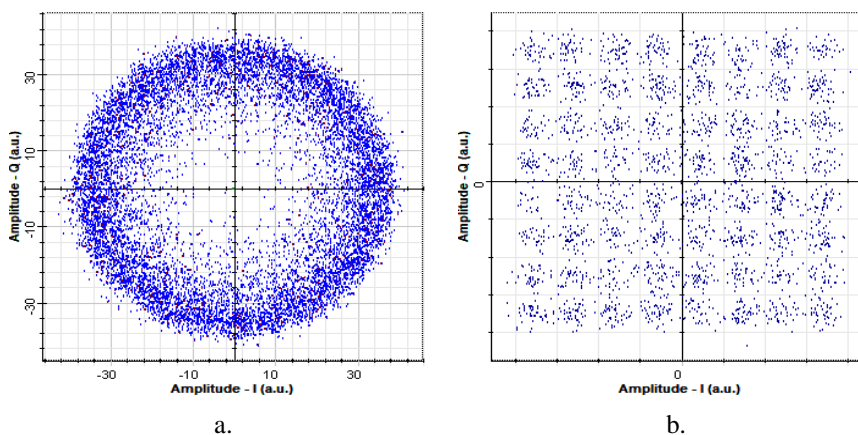
Table 12: Summary of QF and BER for 64-QAM with coherent detection without using DSP compensation

Distance (km)	Quality Factor	Min BER	Log (Min BER)
5	6.48	1.50×10^{-12}	-11.82
10	5.36	0.70×10^{-09}	-9.15
20	4.57	0.91×10^{-06}	-6.04
35	3.45	73.15×10^{-06}	-4.14

Table 13: Summary of QF and BER for 64-QAM with direct detection without using DSP compensation

Distance (km)	Quality Factor	Min BER	Log (Min BER)
5	5.62	5.41×10^{-09}	-8.27
10	4.53	0.19×10^{-06}	-6.72
20	3.67	13.29×10^{-06}	-4.88
35	2.46	0.0003537602	-3.45

The constellation diagram of this system as shown in figure 30. shows a slightly useful demodulated OFDM signal at 5 km with the minimum required BER value of 10^{-9} (5.41×10^{-9}). The signal can be decoded by a user.



a. b.
Figure 30: (a) RF-OFDM signal after dispersion compensation using 64-QAM scheme with direct detection and (b) Carrier Phase Estimation for 64-QAM direct detection without using DSP compensation for 5 km fiber length

IV. CONCLUSION

In this paper, an OFDM based RoF fronthaul system is modelled and investigated for 16-PSK, 16-QAM and 64-QAM modulation schemes in OptiSystem 16. This proposed OFDM based RoF system is investigated for 75 GHz millimeter wave carrier. In this paper, the performance of the mentioned modulation schemes is investigated for both optical coherent and direct detection in terms of QF and BER. This paper however introduces a DSP compensation component in the receiver system to compensate for bit errors. However, the purpose of this paper is to analyze and compare the QF and BER performance of 16-PSK, 16-QAM and 64-QAM modulation schemes when the employed detection systems are configured with or without DSP compensation in the receiver system for a range of fiber length (5 to 35km) and a bit rate of 100 Gbits/s. The simulation results presented in this paper shows that, the optical coherent detection system performs better than the direct detection system. Again, the results show that, employing optical coherent detection in the receiver system with DSP compensation for any of the modulation schemes performs better than direct detection with DSP compensation. However, it could be observed from the tables that, 64-QAM employing coherent detection with DSP compensation performs better with the highest QF and BER values for fiber lengths up to 35 km. In this paper, even though the coherent detection systems perform better than the direct detection systems, we observed some unacceptable QF and BER performance values for both 16-QAM and 16-PSK employing coherent detection with DSP for some range of fiber lengths. Also, we observed that, 16-QAM performs better than 16-PSK for both coherent and direct detection. In this paper, the proposed OFDM-based RoF system has been successfully implemented with DSP compensation to achieve 100 Gbits/s bit rate for 5 to 35 km fiber lengths.

REFERENCES

- [1]. Poomari, S. and Chakrapani, A., 2017. A novel scheme for optical millimeter wave Generation using MZM. *ARPN Journal of Engineering and Applied Sciences*, 21(21), pp.6097-6102.s
- [2]. Muthu, K.E. and Raja, A.S., 2016. Bidirectional MM-Wave Radio over Fiber transmission through frequency dual 16-tupling of RF local oscillator. *Journal of the European Optical Society-Rapid Publications*, 12(1), p.24.
- [3]. Thomas, V.A., El-Hajjar, M. and Hanzo, L., 2015. Millimeter-wave radio over fiber optical upconversion techniques relying on link nonlinearity. *IEEE Communications Surveys & Tutorials*, 18(1), pp.29-53.
- [4]. G. H. Nguyen, B. Cabon, and Y. Le Guennec, "Generation of 60-GHz MB-OFDM signal-over-fiber by up-conversion using cascaded external modulators," *J. Lightw. Technol.*, vol. 27, no. 11, pp. 1496–1502, Jun. 2009.
- [5]. X. Fernando, "Radio over fiber—An optical technique for wireless access," *RyersonCommun.Lab., Toronto,ON,Canada,Oct.2009,IEEE Communications Society Presentation.*
- [6]. V. Thomas, S. Ghafoor, M. El-Hajjar, and L. Hanzo, "A full-duplex diversity-assisted hybrid analogue/digitized radio over fibre for optical/ wireless integration," *IEEE Commun. Lett.*, vol. 17, no. 2, pp. 1–4, Feb. 2013
- [7]. V. A. Thomas, S. Ghafoor, M. El-Hajjar, and L. Hanzo, "Baseband radio over fiber aided millimeter-wave distributed antenna for optical/wireless integration," *IEEE Commun. Lett.*, vol. 17, no. 5, pp. 1012–1015, May 2013.
- [8]. S. Ghafoor and L. Hanzo, "Sub-carrier-multiplexed duplex 64-QAM radio-over-fiber transmission for distributed antennas," *IEEE Commun. Lett.*, vol. 15, no. 12, pp. 1368–1371, Dec. 2011.
- [9]. S. Ghafoor, V.A. Thomas, andL.Hanzo, "Duplexdigitizedtransmission of64-QAMsignalsoverasinglefiberusingasinglepulsedlasersource," *IEEE Commun. Lett.*, vol. 16, no. 8, pp. 1312–1315, Aug. 2012.
- [10]. Hong Wu, Yingxin Zhao, Lijun Ge, Weiyi Tan, Jiajie Yuan. "A Low-Complexity Frequency Offset Correction Scheme for Synchronization in OFDM Systems", 2008 4th International Conference on Wireless Communications, Networking and Mobile Computing, 2008
- [11]. Singh, G. and Alphones, A., 2003, December. OFDM modulation study for a radio-over-fiber system for wireless LAN (IEEE 802.11 a). In Fourth International Conference on Information, Communications and Signal Processing, 2003 and the Fourth Pacific Rim Conference on Multimedia. *Proceedings of the 2003 Joint (Vol. 3, pp. 1460-1464). IEEE.*
- [12]. Li, C., Shao, Y., Wang, Z., Zhou, J., Zhou, Y. and Ma, W., 2016. Optical 64QAM-OFDM transmission systems with different sub-carriers. *Optics and Photonics Journal*, 6(08), p.196
- [13]. Ahmad, S. and Zafrullah, M., 2015. 40 Gb/s 4-QAM OFDM radio over fiber system at 60 GHz employing coherent detection. *Journal of Modern Optics*, 62(4), pp.296-301.
- [14]. Puneet Mittal, Nitesh Singh Chauhan, Anand Gaurav, 2015. Coherent detection optical OFDM system. *International Journal of Scientific Research Engineering & Technology (IJSRET)*, ISSN 2278 – 0882
- [15]. Vibhuti Sharma, Neena Gupta, 2017. Design and Optimization of CPFASK-OFDM BASED Radio over Fiber System. *Global Scientific Journal, GSJ: Volume 5, Issue 11*
- [16]. Khair, F., Fakhriy, H.P., Mustika, I.W., Setiyanto, B. and Idrus, S.M., 2015, October. Modeling and simulation of OFDM scheme for radio over fiber (RoF). In 2015 2nd International Conference on Information Technology, Computer, and Electrical Engineering (ICITACEE) (pp. 376-381). IEEE.
- [17]. Robert I. Killey P. Bayvel Seb J. Savory, G. Gavioli. Electronic compensation of chromatic dispersion using a digital coherent receiver. *Optic Express* 2120, Vol. 15, No. 5, March 2007.